




## Article

# Hydrotalcites with heterogeneous anion distributions: a first approach to producing new materials to be used as vehicles for the successive delivery of compounds

Franchescoli D. Velázquez-Herrera and Geolar Fetter\* 

Benemérita Universidad Autónoma de Puebla, Facultad de Ciencias Químicas, Blvd. 14 Sur y Av. San Claudio, C.P. 72570 Puebla, PUE, Mexico

### ABSTRACT

Hydrotalcites with heterogeneous distributions of anions between their layers were synthesized. Some synthesis parameters were studied to verify their influence on the anionic segregation properties of the hydrotalcites. The nature of the divalent cation and the crystallization method were most relevant. Zinc, in contrast to magnesium, assisted in discriminating carbonates and attracting nitrates to form hydrotalcites with heterogeneous distributions using microwave irradiation. Furthermore, the identification of this kind of hydrotalcite could be easily verified by determining the presence of a double reflection in the 003 X-ray diffraction (XRD) maximum, which definitively characterized a heterogeneous anion distribution. Finally, the reason as to why in some cases the hydrotalcite presented two reflections in the 003 XRD peak was elucidated.

**Keywords:** 003 X-ray diffraction peak, anion segregation, anionic clays, drug delivery, layered double hydroxides, microwave irradiation  
(Received 1 July 2019; revised 10 December 2019; Accepted Manuscript online: 4 February 2020; Associate Editor: Chun Hui Zhou)

Hydrotalcites, also known as layered double hydroxides or double metal hydroxides, are anionic clays with a two-dimensional layered structure, alternating positively charged mixed-metal hydroxide sheets and negatively charged interlayer anions along with water molecules (Gastuche *et al.*, 1967; del Arco *et al.*, 2008; Wang & O'Hare, 2012). They are used in many applications in various fields, such as in catalysis, ion exchange and adsorption (Pérez *et al.*, 2015; Abderrazek *et al.*, 2017; Benedictto *et al.*, 2018; de Castro *et al.*, 2018). More recently, these materials have been employed successfully as vehicles for the controlled delivery of medicines, in which the distribution of the intercalated drug species between the hydrotalcite layers determines its effectiveness (Rives *et al.*, 2014). Some cationic clays may be intercalated with two or more cations whereby each type of cation is segregated in determined diffraction domains of the interlayer space (Zhu *et al.*, 2009). In this case, an easy way to detect whether a solid has this type of intercalation is by analysing the shape of the X-ray diffraction (XRD) peaks. If a 00l peak presents two maxima, each maximum may be correlated with one type of interlayer species. The interlayer distance may define the ion sizes present in the interlayer space and, consequently, their nature (Cavani *et al.*, 1991). In this manner, the distribution of various anions in the hydrotalcite particles may also be estimated.

Although this type of intercalation is known for cationic clays, no reports of this exist for anionic clays. Previous studies (de Roy

*et al.*, 1992; Mantilla *et al.*, 2010; Bhuiyan *et al.*, 2014; Eiby *et al.*, 2016) have reported XRD traces with a 003 peak presenting two maxima, but did not provide a convincing explanation regarding the splitting of the 003 peak. The 003 peak splitting conforming to two maxima may be correlated with a heterogeneous distribution of anions in the interlayer diffraction domain. This heterogeneous anion distribution occurs mainly when zinc is present in the hydrotalcite lamellae (Mantilla *et al.*, 2010; Velázquez-Herrera *et al.*, 2018), but other parameters, such as the precipitating agent employed and the synthesis method, should also be considered (Climent *et al.*, 2004; Sommer *et al.*, 2010). Thus, it will be of interest to clarify why, in some hydrotalcites, the 003 XRD peak presents two reflections and under which conditions this phenomenon occurs. If these conditions are established, new hydrotalcites with segregated anion compounds may be obtained, and therefore many important applications can be envisaged, such as a successive drug-liberation vehicle in the pharmaceuticals field. In this case, a hydrotalcite may be designed to liberate one compound in the first stage and then another, thereby simplifying the normal administration of two compounds successively.

In the present study, hydrotalcites were synthesized with magnesium and/or zinc as divalent cations with trivalent aluminium to study their influence on the splitting of the 003 peak. Nitrates and carbonates were the interlayer anions. The synthesis was performed using three different methods: conventional, ultrasonic and microwave irradiation. The effects of the precipitating agent – sodium or ammonium hydroxides – and the drying temperature were also considered. All of the variations in the hydrotalcite composition and in the synthesis conditions were designed carefully to elucidate the influence of these parameters on the 003 peak reflection doublet and to determine whether

\*Email: [geolarfetter@yahoo.com.mx](mailto:geolarfetter@yahoo.com.mx)

**Cite this article:** Velázquez-Herrera FD, Fetter G (2020). Hydrotalcites with heterogeneous anion distributions: a first approach to producing new materials to be used as vehicles for the successive delivery of compounds. *Clay Minerals* 55, 31–39. <https://doi.org/10.1180/clm.2020.2>

there is a correlation between the distributions of nitrates and carbonates in the hydrotalcite crystals.

## Experimental

### Materials

Magnesium nitrate (Sigma-Aldrich, 99%), zinc and aluminium nitrate (Sigma-Aldrich, 98%) were used as the reactants to synthesize the layered double hydroxides. Sodium hydroxide (Merck, 99%) and ammonium hydroxide (Baker, 28%) were used as precipitating agents.

### Hydrotalcite synthesis

The samples were synthesized by simultaneously dripping a Zn- (or Mg- and Zn-) and Al-nitrate aqueous solution ( $2.5 \text{ mol L}^{-1}$ ) and a sodium or ammonium hydroxide solution ( $2.0$  and  $1.5 \text{ mol L}^{-1}$ , respectively) together in a reaction vessel. The dripping flow for each solution was adjusted to maintain a constant pH of 8. This pH value was selected because the synthesis of Zn/Al hydrotalcites is very dependent on the precipitation pH and should be  $<9$  to obtain almost pure layered double hydroxides (Cavani *et al.*, 1991). The solution amounts corresponded to Zn/Al molar ratios of 2, 3 and 4. When two divalent cations were used in the same sample, resulting in a trimetallic hydrotalcite, the molar amount of each divalent cation was the same (*i.e.* for a molar ratio of  $(\text{Zn} + \text{Mg})/\text{Al} = 2$ , the ratio of Zn/Mg was 1/1). The resulting mixtures were submitted to a crystallization process using three different methods: (1) a microwave autoclave (MIC-I, Sistemas y Equipos de Vidrio S.A. de C.V.) operating at 2.45 GHz and 200 W for 10 min at  $80^\circ\text{C}$ ; (2) an ultrasonic bath (Branson 5510)

operating at 135 W and 50 Hz for 20 min at room temperature; and (3) an open reactor with a conventional heating system at  $80^\circ\text{C}$  with constant stirring for 24 h. After the hydrothermal treatment, the solids were recovered by decantation and washed with distilled water until the pH of the supernatant solution was  $\sim 7$ . Most of the solids were dried at  $70^\circ\text{C}$  for 24 h, but in some cases, where the effect of the drying temperature was studied, the drying varied between  $20^\circ\text{C}$ ,  $40^\circ\text{C}$  or  $60^\circ\text{C}$ . Table 1 summarizes the conditions of synthesis. Another sample was prepared in an inert nitrogen atmosphere using a glove chamber (MAI sample), followed by crystallization *via* microwave irradiation. The washing step was performed as described above, and the drying temperature was  $70^\circ\text{C}$ .

### Characterization methods

#### X-ray diffraction

The XRD traces of the samples were obtained using a Bruker D8 Discover diffractometer with a copper anode X-ray tube, equipped with a Göbel mirror and a LYNXEYE detector. The powder was supported in a polyethylene sample holder. Diffraction data were collected in the Bragg–Brentano  $\theta$ – $2\theta$  geometry. The scanning range was  $5$ – $70^\circ$ , the step size was  $0.025^\circ$  and the scanning time per step was 36 s.

#### Fourier-transform infrared spectroscopy

Fourier-transform infrared (FTIR) spectra were recorded using a Nicolet Magna-IR 550 spectrometer. The solids (11%) were dispersed in KBr to form wafers. The spectra were collected in the  $4000$ – $400 \text{ cm}^{-1}$  infrared region after 32 scans at  $2 \text{ cm}^{-1}$  resolution.

**Table 1.** Hydrotalcite synthesis conditions and the resulting interlayer distances.

Sample	Metal cations	Metallic molar ratio $M^{2+}:\text{Al}$	Crystallization method	Precipitating or exchange agent	Drying temperature ( $^\circ\text{C}$ )	$d_{003}^a$ (Å)	$d_{003}^b$ (Å)
MN2	Zn/Al	2:1	Microwave	NaOH	70	8.8	7.7
MN3	Zn/Al	3:1	Microwave	NaOH	70	8.8	7.6
MN4	Zn/Al	4:1	Microwave	NaOH	70	8.5	7.6
UN2	Zn/Al	2:1	Ultrasound	NaOH	70	8.9	7.7
UN3	Zn/Al	3:1	Ultrasound	NaOH	70	8.9	7.8
UN4	Zn/Al	4:1	Ultrasound	NaOH	70	8.9	8.0
CN2	Zn/Al	2:1	Conventional	NaOH	70	8.9	7.8
CN3	Zn/Al	3:1	Conventional	NaOH	70	8.2	–
CN4	Zn/Al	4:1	Conventional	NaOH	70	8.1	–
MA2	Zn/Al	2:1	Microwave	$\text{NH}_4\text{OH}$	70	8.8	7.6
UA2	Zn/Al	2:1	Ultrasound	$\text{NH}_4\text{OH}$	70	8.9	7.7
CA2	Zn/Al	2:1	Conventional	$\text{NH}_4\text{OH}$	70	8.8	7.7
MN20	Zn/Al	2:1	Microwave	NaOH	20	8.8	7.7
MN40	Zn/Al	2:1	Microwave	NaOH	40	8.7	7.7
MN60	Zn/Al	2:1	Microwave	NaOH	60	8.7	7.8
MA20	Zn/Al	2:1	Microwave	$\text{NH}_4\text{OH}$	20	8.8	7.7
MA40	Zn/Al	2:1	Microwave	$\text{NH}_4\text{OH}$	40	8.8	7.7
MA60	Zn/Al	2:1	Microwave	$\text{NH}_4\text{OH}$	60	8.8	7.7
MAM2	ZnMg/Al	2:1	Microwave	$\text{NH}_4\text{OH}$	70	8.8	7.8
UAM2	ZnMg/Al	2:1	Ultrasound	$\text{NH}_4\text{OH}$	70	8.9	7.8
CAM2	ZnMg/Al	2:1	Conventional	$\text{NH}_4\text{OH}$	70	8.8	7.8
MAI	Zn/Al	2:1	Microwave	$\text{NH}_4\text{OH}$	70	8.8	7.7
MAIC	Zn/Al	2:1	Exchanged	carbonate	25	–	7.6
MAIN	Zn/Al	2:1	Exchanged	nitrate	25	8.8	7.7
MAIcit	Zn/Al	2:1	Exchanged	citrate	25	–	7.7

<sup>a</sup> $d_{003}$  corresponds to the interlayer distance obtained from the 003 XRD peak when only one maximum is observed or when the 003 peak presents two maxima, and the reported value corresponds to the maximum located on the left and can be correlated with intercalated nitrates.

<sup>b</sup> $d_{003}$  corresponds to the interlayer distance obtained when the 003 peak presents two maxima, and the reported value corresponds to the maximum located on the right and can be correlated with intercalated carbonates.

### Scanning electron microscopy

The textures of the synthesized hydroxides were studied on gold-coated samples with a JEOL JSM-6610LV scanning electron microscope (SEM) operating at 15 keV. An X-ray energy-dispersive analysis (EDS) system with an Oxford INCA beryllium detector with a 40 mm window was coupled to the SEM instrument to determine the hydrotalcite composition.

### Inductively coupled plasma optical emission spectrometry

The Zn, Mg and Al contents of the hydrotalcites were determined by inductively coupled plasma optical emission spectrometry (ICP-OES) using a Varian 730-ES ICP-OES device. The samples were prepared by dissolving 1 mg of hydrotalcite powder in 50 mL of 0.48 M HNO<sub>3</sub> solution.

### Nitrogen physisorption

The N<sub>2</sub> adsorption-desorption isotherms were obtained using a Micromeritics ASAP 2020 instrument at -198°C. Prior to analysis, the samples were outgassed in vacuum at 150°C overnight. The outgassing conditions ensured that the hydrotalcite was fully dehydrated and that the structure was maintained. The specific surface areas were determined using the Brunauer-Emmett-Teller (BET) equation.

## Results and discussion

### Crystallization method and the Zn/Al molar ratio effects

Figure 1 shows the XRD traces of the Zn/Al samples precipitated with NaOH at metallic molar ratios of 2, 3 and 4 and crystallized using the conventional, microwave and ultrasonic irradiation methods. All of the samples show the (003), (006), (009), (012), (110) and (113) peaks characteristic of hydrotalcites, in accordance with JCPD card 00-014-0191. In the MN3, MN4 and UN4

samples, the presence of low-intensity reflection peaks at 32, 34 and 36°2θ indicates the presence of small amounts of zinc oxide (zincite) impurities. The zincite is formed at higher metallic molar ratios; zinc cations might be concentrated near the exterior part of the crystals and, under microwave or ultrasound, might form zinc oxide (Rivera *et al.*, 2006). When the intensities of the (110) and (113) peaks are considered, the most intense peaks correspond to the samples synthesized using the conventional method at metallic molar ratios of 3 and 4, denoted as the CN3 and CN4 samples. This indicates that the conventional method promotes a more regular accommodation of the cations in the hydrotalcite lamellae compared to the microwave or ultrasound methods (Lobo-Sánchez *et al.*, 2018). However, a noise increase in the CN samples indicates a reduction in crystal order from CN2 to CN4, and a less visible effect is observed for the MN and UN series.

The samples synthesized with a metallic molar ratio of 3 presented more regular 00l peaks, independent of the synthesis method (Rivera *et al.*, 2006; Xie *et al.*, 2006). By contrast, samples crystallized in the presence of microwaves or ultrasound at molar ratios of 2 or 4 show two maxima in the 003 and 006 peaks or a shoulder at the right-hand side of the 003 peak. The corresponding interlayer distances (calculated using the Bragg equation), based on the positions of the two 003 peak maxima, are reported in Table 1. The resulting interlayer distances of 8.8 and 7.7 Å are attributed to interlayered nitrate and carbonate species, respectively (Cavani *et al.*, 1991). Thus, when these anionic species are distributed heterogeneously within the hydrotalcite crystals, two different diffraction domains are expected: one associated with the carbonates and the other with the nitrates. When the 003 and 006 peaks are symmetrical (*i.e.* with one maximum only), the anion distribution is homogeneous and the resulting interlayer distance is ~8.2 Å; this value is the average of the interlayer distances corresponding to the nitrates and carbonates, as in the

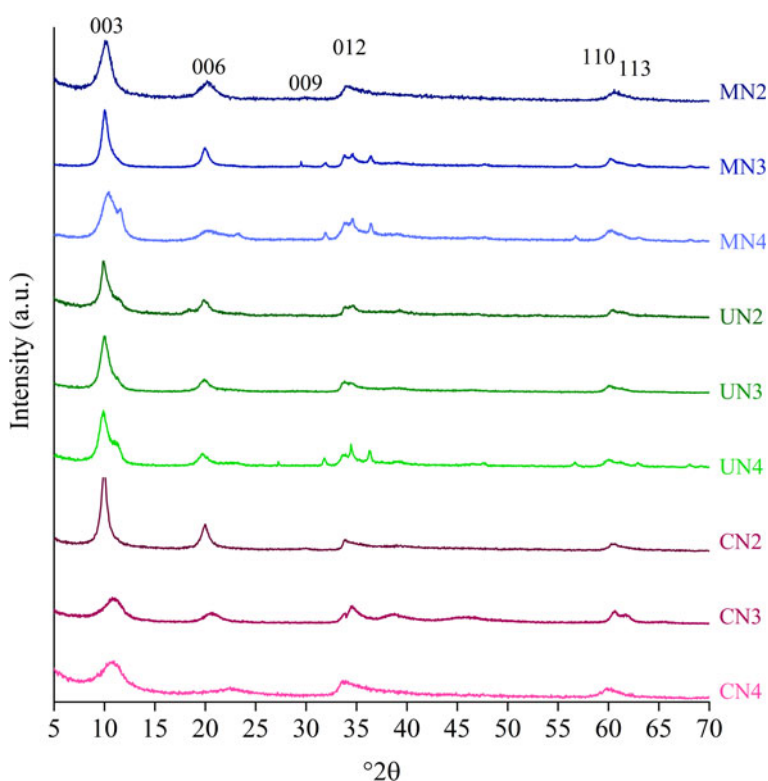


Fig. 1. XRD traces of the Zn/Al samples precipitated with NaOH at metallic molar ratios of 2, 3 and 4 and crystallized using the conventional, microwave and ultrasonic irradiation methods.

CN3 and CN4 samples (Sommer *et al.*, 2010). In addition, a comparison of the 003 peak splitting intensities suggests that microwaves promoted the best anion segregation in the hydrotalcite crystals (MN4 sample), followed by a sample treated using ultrasound (UN4).

Thus, from the XRD results, it can be concluded that the most effective method for promoting anion segregation is microwave irradiation, followed by ultrasound and then by conventional treatment. These differences in ion distribution can be attributed to the ion mobility in the reaction medium and the sizes and charges of the ions. Ultrasonic waves have large wavelengths and scarcely increase ion mobility, unlike microwaves. The only effect on hydrotalcite synthesis promoted by ultrasound is the high pressure and temperature derived from the cavitation phenomenon (Paredes-Carrera *et al.*, 2015). Thus, the use of ultrasound is expected to have only a small effect on anionic segregation. The synthesis carried out using the conventional method, where slow crystallization occurs, contributes to the homogeneous anion arrangement. In this case, the ion mobility is too slow to influence the ion size and charge, and thus a homogeneous dispersion of metallic cations and anions in the hydrotalcite network may be achieved. The efficiency of the microwave method may be attributed to the wavelength being close to the size of the ions. Thus, the microwaves increase ion diffusion and favour a more rapid integration of those hydrotalcite nuclei with small sizes and high charges than those that are less charged and larger. Indeed, previous work has demonstrated that in Mg/Al hydrotalcites there is an enrichment of the trivalent cation at the core of the particles when the synthesis is conducted in the presence of microwave irradiation, showing that aluminium diffuses more rapidly than zinc cations (de la Hoz *et al.*, 2005; Rivera *et al.*, 2006; Gupta *et al.*, 2018). Thus, the hydrotalcite particles display a composition gradient whereby the core is aluminium-enriched and the exterior is more concentrated in zinc cations. Furthermore, Britto *et al.* (2007) reported that zinc cations have a better affinity for nitrates than for carbonates through testing the thermal stability of hydrotalcites. A greater stability was observed for the nitrated zinc-containing hydrotalcites than the carbonated zinc materials. Those authors attributed the greater observed stability to the difference in the coordination mode of the zinc with nitrates.

Carbonates are known to intercalate with their plane perpendicular to the *c*-axis of the hydrotalcite layers, while nitrates intercalate with one of the NO bonds collinear with the *c*-axis, ensuring better coupling between ions (Xu & Zeng, 2001).

Regarding the Zn/Al metallic molar ratio, anion segregation is more noticeable with molar ratios of 2 or 4. Hydrotalcites with a molar ratio of 3 are more crystalline than those with other ratios (Olszówka *et al.*, 2018). The cation and anion distributions are more regular throughout the solid, and consequently segregation cannot be produced.

#### Drying temperature effect

The hydrotalcite drying temperature was varied to determine its influence on the splitting of the 003 and 006 diffraction peaks in the case of a crystal symmetry change (de Roy *et al.*, 1992). The microwave method was chosen because it promotes anion segregation. Figure 2 displays the XRD traces of samples prepared with either ammonium or sodium nitrates at a metallic molar ratio of 2 with drying temperatures of 20°C, 40°C and 60°C and drying times of up to 3 days. The molar ratio of 2 was selected because it promotes a greater layer charge, and consequently a large number of interlayered anions are present, which may result in easier segregation. In addition, at this ratio, zincite formation may be avoided. All diffraction traces were similar; the splitting of the 003 peak was not well defined, but due to the width and asymmetry, the presence of two peaks may be inferred. The boundary between cations is less evident in this case. Hence, the drying temperature did not modify the anion distribution.

#### Precipitating agent effect

To determine the influence of the precipitating agent on anion segregation, Zn/Al hydrotalcites with a molar ratio of 2 were synthesized with either ammonium or sodium hydroxide using the conventional, microwave and ultrasonic methods. The XRD traces of the samples prepared with ammonium are presented in Fig. 3. Two distinct maxima were detected clearly in the MA2 and CA2 samples, corresponding to the 003 and 006 peaks. This indicates that ammonium hydroxide, with a Zn/Al

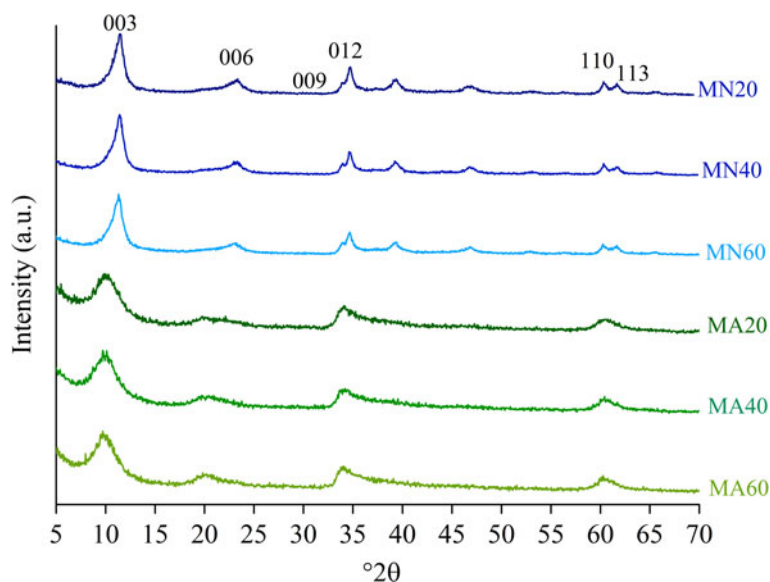


**Fig. 2.** XRD traces of the samples prepared with  $\text{NH}_4\text{OH}$  or  $\text{NaOH}$  as precipitating agents at a metallic molar ratio of 2 and crystallized using microwave irradiation and dried at 20°C, 40°C and 60°C.

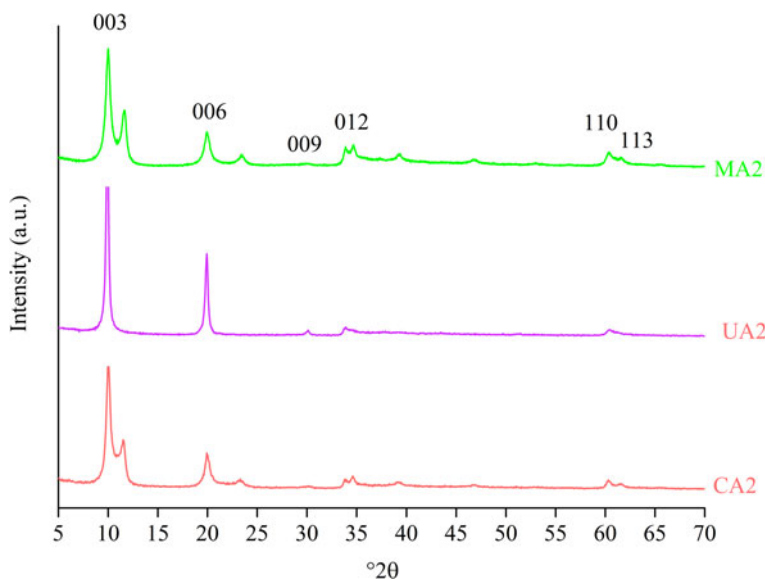


**Fig. 3.** XRD traces of the Zn/Al samples prepared with  $\text{NH}_4\text{OH}$  as a precipitating agent at a metallic molar ratio of 2 and crystallized using the conventional, ultrasound and microwave irradiation methods.

composition and a molar ratio of 2, promotes the best segregation of nitrates and carbonates. By contrast, with sodium hydroxide, only a shoulder was observed, indicative of a less intense anion segregation (Fig. 1).

The cations originating in sodium and ammonium reactants do not form part of the hydrotalcite structure, but they are present in the reaction medium and may obstruct the diffusion of the cations that do form the hydrotalcite structure.  $\text{NH}_4^+$ , which is larger than the Na ion, may obstruct the movement of larger ions with higher charge, but not those ions that are smaller and/or have lower charge (Rocha Oliveira *et al.*, 2015). Thus, in the presence of ammonium, both aluminium and carbonates are concentrated in the cores of the particles.

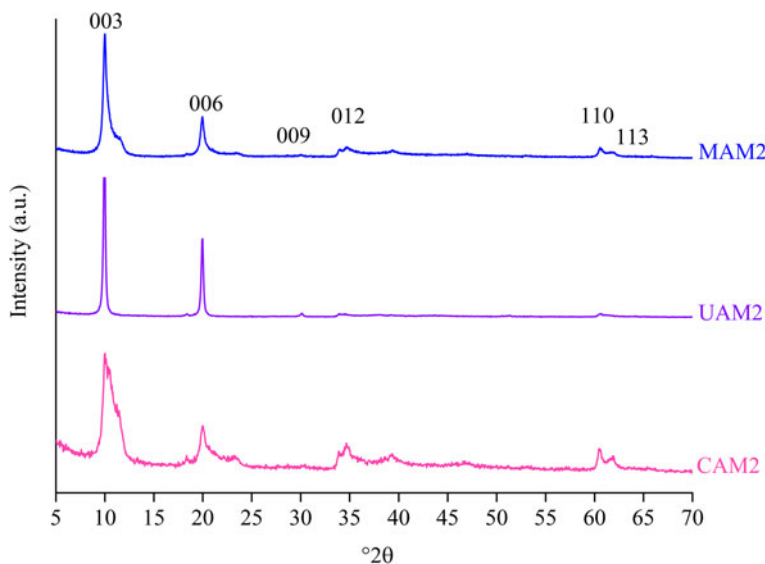
#### Magnesium addition effect on the Zn/Al hydrotalcites

Figure 4 shows the XRD traces of the trimetallic ZnMg/Al hydrotalcite samples synthesized with ammonium hydroxide in the presence of microwaves or prepared using the conventional

method (samples MAM2 and CAM2). The traces show a diminution in the splitting of the 003 peak compared to that of the corresponding samples without Mg (MA2 and CA2 samples in Fig. 3). It can be concluded that the Mg cations do not promote anion segregation. Instead, they stimulate a homogeneous distribution of the nitrates and carbonates, as previously reported in similar studies (Bergadà *et al.*, 2007; Sommer *et al.*, 2010). Thus, Zn has a strong effect and is responsible for the anion arrangement within the nitrate diffraction domains. Most likely, Zn cations tend to cluster due to their *d*-orbitals; they are not present in the Mg samples, and consequently Mg is distributed homogeneously within the sheets.

#### Effect of an inert atmosphere on synthesis

A zinc and aluminium reactant solution at amounts corresponding to a molar ratio of 2 was co-precipitated with a solution of  $\text{NH}_4\text{OH}$  in a glove chamber under an inert atmosphere of nitrogen, to avoid the formation of carbonates in the synthesis medium



**Fig. 4.** XRD traces of the ZnMg/Al samples prepared with  $\text{NH}_4\text{OH}$  as a precipitating agent at a metallic molar ratio of 2 and crystallized using the conventional, ultrasound and microwave irradiation methods.

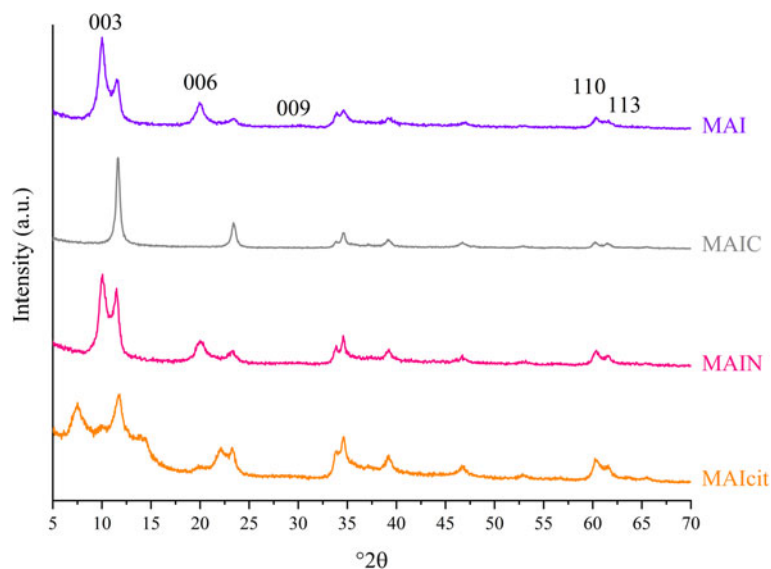


**Fig. 5.** XRD traces of the samples prepared under an inert nitrogen atmosphere (MAI) and exchanged with carbonates (MAIC), nitrates (MAIN) and citrates (MAIcit).

from the  $\text{CO}_2$  present in the air, which would occupy the nitrate positions in the interlayer space. The hydrothermal treatment was performed by microwave irradiation. The XRD trace of this sample, labelled as MAI, displays splits of the 003 and 006 peaks (Fig. 5). Thus, it may be assumed that the two maxima in the 003 peak correspond to carbonates and nitrates intercalated in various diffraction domains of the solid; the maximum at  $11.5^\circ 2\theta$  corresponds to carbonates, and that at  $10^\circ 2\theta$  corresponds to nitrates (Cavani *et al.*, 1991). This indicates that even when the precipitation process was carried out under an inert atmosphere, carbonates are present in the resulting hydrotalcite. These carbonate anions were incorporated during the microwave crystallization treatment that was conducted in a  $\text{CO}_2$  atmosphere. The presence of interlayered carbonates and nitrates was also confirmed by FTIR spectroscopy from the presence of a band at  $\sim 1382 \text{ cm}^{-1}$  (Fig. 6), but this technique cannot differentiate their amounts or their locations in the interlayer diffraction domains of the solid.

#### Anion exchange effect

To verify that the two maxima of the 003 diffraction peak correspond to a hydrotalcite with a diffraction domain conformed by carbonates separately from that containing nitrates, two exchange processes were performed on the MAI sample at room temperature under stirring for 24 h: one dispersing an amount of MAI hydrotalcite in water containing carbonates and the other containing nitrates, producing samples labelled MAIC and MAIN, respectively. The solids were washed with deionized water and dried at  $70^\circ\text{C}$ .

The 003 peak at  $10^\circ 2\theta$  and the 006 peak disappear from the XRD traces of the MAIC hydrotalcite sample exchanged with carbonates (Fig. 5). Hydrotalcites have a much greater affinity for carbonates than for nitrates (Balcomb *et al.*, 2015). It is very difficult to synthesize a hydrotalcite that is free of carbonates (Iyi *et al.*, 2004; Ay *et al.*, 2007). Thus, in the MAIC sample,

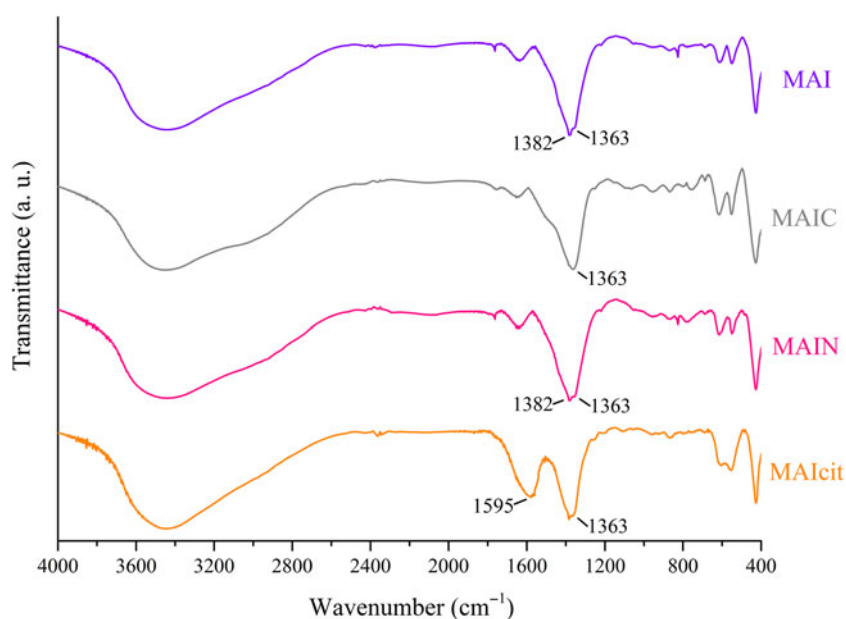


**Fig. 6.** FTIR spectra of the samples prepared under an inert nitrogen atmosphere (MAI) and exchanged with carbonates (MAIC), nitrates (MAIN) and citrates (MAIcit).

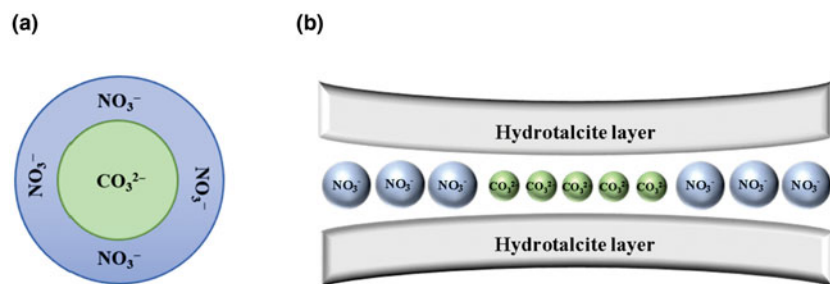


Fig. 7. Schematic representation of a hydrotalcite with a heterogeneous anion distribution: (a) top view and (b) front view.

carbonates displaced all of the interlayered nitrates to form a completely carbonated hydrotalcite with an interlayer distance of 7.7 Å. In addition, the FTIR spectrum of this sample shows a band centred at  $1363\text{ cm}^{-1}$ , corresponding to interlayered carbonates (Lennerová *et al.*, 2015). When the MAI sample was exchanged with nitrates to form the MAIN hydrotalcite, the 003 peak had two maxima, indicating, as expected, that nitrates did not displace the interlayered carbonates. Furthermore, from the peak intensities it can be inferred that, during the exchange, more carbonates were incorporated into the hydrotalcite interlayer. The FTIR spectrum of this sample also displays the presence of both anions *via* a band centred at  $1382\text{ cm}^{-1}$  (Fig. 6) (Rocha Oliveira *et al.*, 2015).

A scheme for the structure of a Zn/Al hydrotalcite with anion segregation is shown in Fig. 7. The crystal core contains Al enriched with segregated interlayered carbonates, and the crystal shell contains zinc enriched with segregated nitrates. This scheme is supported by the elemental chemical analysis results for the MAI, MAIC and MAIN samples (Table 2). The amounts of carbon and nitrogen may be correlated with the abundance of carbonates and nitrates, respectively. The MAI sample had 6.0 wt.% carbon and 3.6 wt.% nitrogen, indicating that it contained carbonates even when the sample was prepared in an inert atmosphere, as is also shown by XRD analysis. When the MAI sample was exchanged with carbonates to form the MAIC hydrotalcite, the amount of carbon increased to 22.0 wt.%, while the nitrogen percentage was zero. This is to be expected, as carbonates displace nitrates (Ay *et al.*, 2007). When the MAI sample was exchanged with nitrates, the amount of carbon increased to 18.3 wt.%, but the amount of nitrogen remained essentially unchanged (2.7 wt.%), confirming that the nitrates hardly displace the carbonates. The Zn/Al molar ratios of the MAI samples obtained by EDS analysis (Table 2) decreased from 2.4 to 2.2 and 2.0 after the exchange with carbonates or nitrates, respectively. The Zn/Al molar ratios of the three samples obtained by ICP-OES were virtually constant, varying from 1.7 to 1.8, being slightly lower

than the nominal value of 2.0. Considering that the EDS technique determines the elemental composition near the surface of the solid (Haley *et al.*, 2006), it may be inferred from the zinc content (Table 2) that an enrichment of zinc occurs more notably for the MAI sample, which is less intense for the MAIC hydrotalcite, and even less than that for the MAIN hydrotalcite.

The reduction of the surface zinc content for the exchanged samples may be attributed to the decomposition of the rims of the hydrotalcite particles when the sample is placed in an acidic exchange medium with a pH of 5.7. During 24 h of ionic exchange, only a small part of the hydrotalcite surface was decomposed. In this manner, the superficial zinc was dissolved during washing, thereby decreasing its abundance in the solid, in accordance with the decrease of the Zn/Al molar ratios of the exchanged samples. This is in agreement with the XRD results with regards to the relative intensities of the two maxima in the 003 peak. The maximum corresponding to nitrates in the MAI sample is three times more intense than the maximum corresponding to carbonates, while for the MAIN sample, the intensities of the two maxima were comparable, indicating a reduction of the nitrate content. Inayat *et al.* (2011) also reported a change in the 003 peak from a singlet at  $10^\circ 2\theta$  corresponding to interlayered nitrates into a doublet with maxima at  $10$  and  $11.4^\circ 2\theta$  when the nitrates were partially replaced by carbonates, and finally into a single peak at  $11.4^\circ 2\theta$  after complete exchange of nitrates by carbonates. These results indicate a heterogeneous anion distribution when the 003 peak is composed of a doublet. In addition, the results of the specific surface area (Table 2) are also in accordance with the anion heterogeneity. The MAI and MAIN samples presented very low surface areas of  $\sim 3.9\text{ m}^2\text{ g}^{-1}$ , while the MAIC sample had a higher value of  $27.7\text{ m}^2\text{ g}^{-1}$ . Nitrated hydrotalcites have surface areas of  $<15\text{ m}^2\text{ g}^{-1}$  (Fetter *et al.*, 2000).

To confirm the heterogeneous anion distribution, another anionic exchange was performed with citrate ions because nitrate ions located on the rim are exchangeable, whereas carbonate ions in the core are not. This exchange was conducted by mixing a

Table 2. Elemental composition (wt.%) obtained by EDS and by ICP-OES, the resulting metallic molar ratios and the specific surface areas of the hydrotalcite samples.

Sample	Elemental composition obtained by EDS (wt.%)				Zn/Al molar ratio obtained by EDS	Elemental composition obtained by ICP-OES (wt.%)		Zn/Al molar ratio obtained by ICP-OES	Specific surface area ( $\text{m}^2\text{ g}^{-1}$ )
	C	N	Zn	Al		Zn	Al		
MAI	6.0	3.6	38.0	6.5	2.4	33.6	7.8	1.8	3.9
MAIC	22.0	0.1	25.5	4.8	2.1	40.8	9.6	1.7	27.7
MAIN	18.3	2.7	25.4	5.1	2.0	33.7	8.1	1.7	3.8
MAIcit	34.4	0.2	20.1	3.7	2.2	32.8	7.7	1.8	1.2

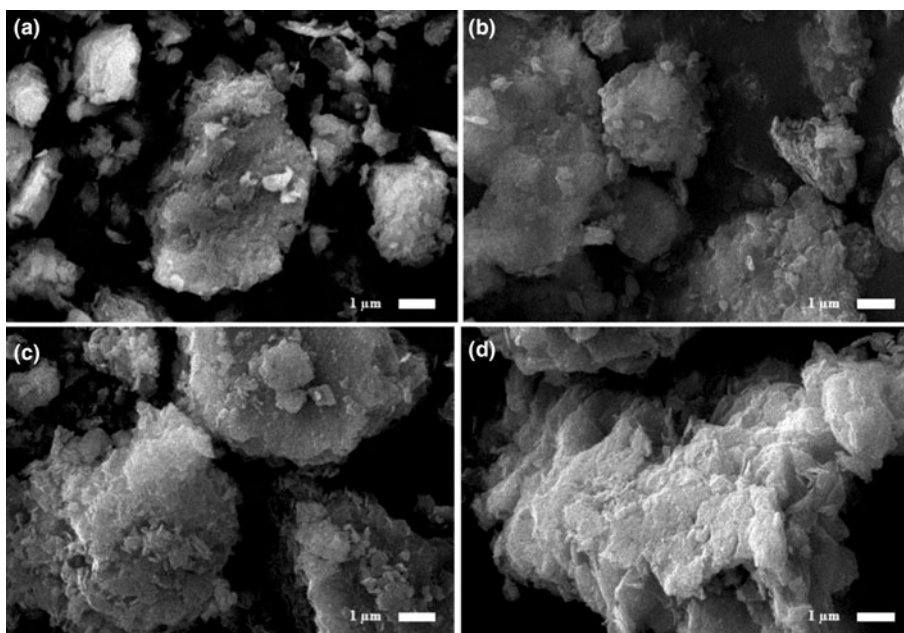


**Fig. 8.** SEM images of (a) MAI, (b) MAIC, (c) MAIN and (d) MAIcit hydrotalcites.

sodium citrate solution with an MAI sample to form an MAIcit sample. The exchange process was performed at room temperature with stirring for 2 h. Due to the larger size of the citrate anions, the corresponding 003 and 006 XRD peaks should be observed at a smaller angle than their nitrate counterparts (Li & Kirkpatrick, 2007). The new diffraction peaks appeared at  $7.4$  and  $14.8^\circ 2\theta$ , corresponding to the 003 and 006 planes of the citrate intercalated hydrotalcite (MAIcit), resulting in a  $d_{003}$  of  $11.8 \text{ \AA}$ , thus showing that the citrates exchange with the nitrates (Fig. 5). By contrast, the peaks corresponding to the carbonates remained unchanged. The results of the FTIR, EDS and nitrogen physisorption analyses also confirm that citrates replaced the nitrates but not the carbonates. The FTIR spectrum of the MAIcit sample shows the presence of the carbonate band centred at  $1363 \text{ cm}^{-1}$  and a new band corresponding to the citrate ions due to the C=O bonds of the carboxylate groups at  $1595 \text{ cm}^{-1}$  (Tran *et al.*, 2018), which overlaps with adsorbed water.

The MAIcit sample has a lower specific surface area of  $1.2 \text{ m}^2 \text{ g}^{-1}$ , indicating that citrate anions promote a denser agglomeration of particles. The EDS analysis shows a carbon content of 34.4 wt.% for the MAIcit sample, which is much larger than those of the other samples. When compared to the MAIC hydrotalcite, an increase of 64% was observed in terms of the carbon content, which corresponds to the amount of carbon of the remaining carbonates plus that corresponding to the citrate compounds. As expected, nitrates were present in very small amounts.

The structural differences observed under the SEM might also help us to elucidate the anion segregation. Figure 8 compares the morphology of the MAI sample with its exchanged MAIC, MAIN and MAIcit counterparts. The morphologies of the samples having mostly one anionic compound (*i.e.* nitrates in MAI or carbonates in MAIC), displaying the features typically reported for hydrotalcites (*i.e.* a rather dense material conformed by particles forming chunks with heterogeneous sizes) (Rocha Oliveira *et al.*, 2015). Typical flakes are hardly observed. In contrast, for the exchanged MAIN and MAIcit samples, some irregular arrangements are observed in the stacked flakes. The anion segregation may cause such an arrangement, and the separation of the flakes

may be more pronounced when the resulting interlayer distances from one anion to another are larger, as is the case for the MAIcit sample. Hence, this technique also contributes to helping us to differentiate whether a sample has anion segregation.

## Conclusion

Hydrotalcites with heterogeneous anion distributions were synthesized. The main parameters that influence anion segregation are the synthesis method and the nature of the divalent cation. Zinc and microwave irradiation favoured the formation of an anion-segregated hydrotalcite. Ammonium hydroxide, used as a precipitating agent, also contributed to anion segregation. Crystallization performed by microwave irradiation promoted the diffusion of aluminium and carbonate ions to the core, while zinc and nitrate ions remained in the external parts of the hydrotalcite crystals. In addition, zinc has greater affinity for nitrates than carbonates, contributing to the formation of a nitrated phase. Thus, the resulting hydrotalcite is enriched by carbonates in the core and by nitrates in the margins of the crystals.

Furthermore, this work provides a simple way to identify hydrotalcites with anion-segregation properties by observing a splitting in the 003 XRD peak, clarifying why a 003 peak doublet is observed in some hydrotalcites. Finally, hydrotalcites with anion-segregation properties have many potential applications, such as in the pharmaceuticals industry, where they might act not only as a known material with properties of programmed or controlled drug liberation, but also as a vehicle for the release of drugs (*i.e.* drug liberation in stages).

**Acknowledgements.** The authors thank colleagues at the Centro Universitario de Vinculación y Transferencia de Tecnología (CUVYT) for performing some of the technical analyses. FDV-H thanks the Consejo Nacional de Ciencia y Tecnología (CONACYT) for the fellowship.

**Financial support.** The authors acknowledge the Vicerrectoría de Investigación y Estudios de Posgrado – Benemérita Universidad Autónoma de Puebla (VIEP-BUAP) for financial support.



## References

- Abderrazek K., Srasra N.F. & Srasra E. (2017) Photocatalytic decolourization of methylene blue using [Zn–Al] layered double hydroxides synthesized at different molar cationic ratios. *Clay Minerals*, **52**, 203–215.
- Ay A.N., Zümreoglu-Karan B. & Temel A. (2007) Boron removal by hydrotalcite-like, carbonate-free Mg–Al–NO<sub>3</sub>–LDH and a rationale on the mechanism. *Microporous and Mesoporous Materials*, **98**, 1–5.
- Balcomb B., Singh M. & Singh S. (2015) Synthesis and characterization of layered double hydroxides and their potential as nonviral gene delivery vehicles. *Chemistry Open*, **4**, 137–145.
- Benedictto G.P., Sotelo R.M., Dalla Costa B.O., Fetter G. & Basaldella E.I. (2018) Potassium-containing hydroxylated hydrotalcite as efficient catalyst for the transesterification of sunflower oil. *Journal of Materials Science*, **53**, 12828–12836.
- Bergadà O., Vicente I., Salagre P., Cesteros Y., Medina F. & Sueiras J.E. (2007) Microwave effect during aging on the porosity and basic properties of hydrotalcites. *Microporous and Mesoporous Materials*, **101**, 363–373.
- Bhuiyan M.M.R., Lin S.D. & Hsiao T.C. (2014) Effect of calcination on Cu–Zn-loaded hydrotalcite catalysts for C–C bond formation derived from methanol. *Catalysis Today*, **226**, 150–159.
- Britto S., Radha A. V., Ravishankar N. & Kamath P.V. (2007) Solution decomposition of the layered double hydroxide (LDH) of Zn with Al. *Solid State Sciences*, **9**, 279–286.
- Cavani F., Trifirò F. & Vaccari A. (1991) Hydrotalcite-type anionic clays: preparation, properties and applications. *Catalysis Today*, **11**, 173–301.
- Climet M.J., Corma A., Iborra S., Epping K. & Veltz A. (2004) Increasing the basicity and catalytic activity of hydrotalcites by different synthesis procedures. *Journal of Catalysis*, **225**, 316–326.
- de Castro G.F., Ferreira J.A., Eulálio D., de Souza S.J., Novais S.V., Novais R.F., Pinto F.G. & Tronto J. (2018) Layered double hydroxides: matrices for storage and source of boron for plant growth. *Clay Minerals*, **53**, 79–89.
- de la Hoz A., Díaz-Ortiz Á. & Moreno A. (2005) Microwaves in organic synthesis. Thermal and non-thermal microwave effects. *Chemical Society Reviews*, **34**, 164–178.
- de Roy A., Forano C., el Malki K. & Besse J.-P. (1992) Anionic clays: trends in pillaring chemistry. Pp. 108–169 in *Expanded Clays and Other Microporous Solids*, 1st edition (M.L. Occelli & H. Robson, editors). Springer US, New York, NY, USA.
- del Arco M., Fernández A., Martín C., Sayalero M.L. (2008) Solubility and release of fenamates intercalated in layered double hydroxides. *Clay Minerals*, **43**, 255–265.
- Eiby S.H.J., Tobler D.J., Nedel S., Bischoff A., Christiansen B.C., Hansen A.S., Kjaergaard H.G. & Stipp S.L.S. (2016) Competition between chloride and sulphate during the reformation of calcined hydrotalcite. *Applied Clay Science*, **132–133**, 650–659.
- Fetter G., Olguín M.T., Bosch P. & Bulbulian S. (2000) Surface areas of nitrated hydrotalcites. *Journal of Porous Materials*, **7**, 469–473.
- Gastuche M.C., Brown G. & Mortland M.M. (1967) Mixed magnesium–aluminium hydroxides. I. Preparation and characterization of compounds formed in dialysed systems. *Clay Minerals*, **7**, 177–192.
- Gupta P., Behera B., Chhibber V.K. & Ray S.S. (2018) Microwave assisted synthesis of glycerol carbonate over zinc incorporated mesoporous hydrotalcite catalyst. *Current Microwave Chemistry*, **5**, 13–22.
- Haley S.M., Tappin A.D., Bond P.R. & Fitzsimons M.F. (2006) A comparison of SEM-EDS with ICP-AES for the quantitative elemental determination of estuarine particles. *Environmental Chemistry Letters*, **4**, 235–238.
- Inayat A., Klumpp M. & Schwieger W. (2011) The urea method for the direct synthesis of ZnAl layered double hydroxides with nitrate as the interlayer anion. *Applied Clay Science*, **51**, 452–459.
- Iyi N., Matsumoto T., Kaneko Y. & Kitamura K. (2004) Deintercalation of carbonate ions from a hydrotalcite-like compound: enhanced decarbonation using acid-salt mixed solution. *Chemistry of Materials*, **16**, 2926–2932.
- Lennerová D., Kovanda F. & Brožek J. (2015) Preparation of Mg–Al layered double hydroxide/polyamide 6 nanocomposites using Mg–Al-taurate LDH as nanofiller. *Applied Clay Science*, **114**, 265–272.
- Li Q. & Kirkpatrick R.J. (2007) Organic anions in layered double hydroxides: an experimental investigation of citrate hydrotalcite. *American Mineralogist*, **92**, 397–402.
- Lobo-Sánchez M., Nájera-Meléndez G., Luna G., Segura-Pérez V., Rivera J.A. & Fetter G. (2018) ZnAl layered double hydroxides impregnated with eucalyptus oil as efficient hybrid materials against multi-resistant bacteria. *Applied Clay Science*, **153**, 61–69.
- Mantilla A., Tzompantzi F., Fernández J.L., Díaz Góngora J.A.I. & Gómez R. (2010) Photodegradation of phenol and cresol in aqueous medium by using Zn/Al + Fe mixed oxides obtained from layered double hydroxides materials. *Catalysis Today*, **150**, 353–357.
- Olszówka J.E., Karcz R., Bielańska E., Kryściak-Czerwenka J., Napruszewska B.D., Sulikowski B., Socha R.P., Gawel A., Bahranowski K., Olejniczak Z. & Serwicka E.M. (2018) New insight into the preferred valency of interlayer anions in hydrotalcite-like compounds: the effect of Mg/Al ratio. *Applied Clay Science*, **155**, 84–94.
- Paredes-Carrera S.P., Valencia-Martínez R.F., Valenzuela-Zapata M.A., Sánchez-Ochoa J.C. & Castro-Sotelo L. V. (2015) Study of hexavalent chromium sorption by hydrotalcites synthesized using ultrasound vs microwave irradiation. *Revista Mexicana de Ingeniería Química*, **14**, 429–436.
- Pérez E., Ayele L., Getachew G., Fetter G., Bosch P., Mayoral A. & Díaz I. (2015) Removal of chromium (VI) using nano-hydrotalcite/SiO<sub>2</sub> composite. *Journal of Environmental Chemical Engineering*, **3**, 1555–1561.
- Rivera J.A., Fetter G. & Bosch P. (2006) Microwave power effect on hydrotalcite synthesis. *Microporous and Mesoporous Materials*, **89**, 306–314.
- Rives V., del Arco M. & Martín C. (2014) Intercalation of drugs in layered double hydroxides and their controlled release: a review. *Applied Clay Science*, **88–89**, 239–269.
- Rocha Oliveira G., Dias do Amaral L.J., Giovanela M., da Silva Crespo J., Fetter G., Rivera J.A., Sampieri A. & Bosch P. (2015) Bactericidal performance of chlorophyllin–copper hydrotalcite compounds. *Water, Air, & Soil Pollution*, **226**, 226–316.
- Sommer A., Fetter G., Bosch P. & Lara V.H. (2010) New template effect in hydrotalcite synthesis. nodular vs layered morphologies. *Clays and Clay Minerals*, **58**, 340–350.
- Tran H.N., Lin C.C., Woo S.H. & Chao H.P. (2018) Efficient removal of copper and lead by Mg/Al layered double hydroxides intercalated with organic acid anions: adsorption kinetics, isotherms, and thermodynamics. *Applied Clay Science*, **154**, 17–27.
- Velázquez-Herrera F.D., Fetter G., Rosato V., Pereyra A.M. & Basaldella E.I. (2018) Effect of structure, morphology and chemical composition of Zn–Al, Mg/Zn–Al and Cu/Zn–Al hydrotalcites on their antifungal activity against *A. niger*. *Journal of Environmental Chemical Engineering*, **6**, 3376–3383.
- Wang Q. & O'Hare D. (2012) Recent advances in the synthesis and application of layered double hydroxide (LDH) nanosheets. *Chemical Reviews*, **112**, 4124–4155.
- Xie X., Ren X., Li J., Hu X. & Wang Z. (2006) Preparation of small particle sized ZnAl-hydrotalcite-like compounds by ultrasonic crystallization. *Journal of Natural Gas Chemistry*, **15**, 100–104.
- Xu Z.P. & Zeng H.C. (2001) Abrupt structural transformation in hydrotalcite-like compounds Mg<sub>1-x</sub>Al<sub>x</sub>(OH)<sub>2</sub>(NO<sub>3</sub>)<sub>x</sub>·nH<sub>2</sub>O as a continuous function of nitrate anions. *Journal of Physical Chemistry B*, **105**, 1743–1749.
- Zhu R., Wang T., Ge F., Chen W. & You Z. (2009) Intercalation of both CTMAB and Al<sub>13</sub> into montmorillonite. *Journal of Colloid and Interface Science*, **335**, 77–83.